

# Measurement-based Characterization of Human Body Impact on Ultra-low UAV-to-Ground Channels

Mahmoud Badi, Dinesh Rajan, and Joseph Camp  
Southern Methodist University  
Email: {mbadi, rajand, camp}@smu.edu

**Abstract**—At ultra-low altitudes, an unmanned aerial vehicle (UAV) can act as a personal base station, where it communicates only with one user, as in the case of a UAV-assisted soldier. User equipment (UE) can be inside the pocket of a user or near their chest while facing or facing-away from the UAV. In these scenarios, the wireless channel can experience different fading levels based on the UAV's hovering position, user orientation, location of the UE near the user's body, and carrier frequency of the transmitted signal. In this work, we provide measurement results and study how the human body affects the Air-to-Ground (AtG) channel characteristics under various use cases of holding a UE device. These channel characteristics include the average signal strength, shadowing, and Rician K-factor. We target three different ways in which the device is held by the user: Near-Chest Facing, In-pocket Facing, and Near-Chest Facing-away from the transmitting UAV. We perform this study at carrier frequencies of 900 MHz and 2.5 GHz and in Line-of-Sight (LOS) conditions. First, we conduct a set of baseline experiments to understand AtG channels in free space with no human involved. Second, we conduct AtG experiments with the user holding the device and show that the human body can induce either gains or losses compared to free space, depending on the user orientation with respect to the UAV. Third, we find that there are two distinct regions of operation, one in which the channel characteristics are mainly affected by the UAV and another that is dominated by the user's body. The obtained results help create more realistic 3D UAV-to-ground channel models and complement adaptive aerial drone deployment algorithms that target making intelligent decisions about trajectory and energy consumption when considering human body effects.

**Index Terms**—Air-to-Ground Channels, UAVs, Drones, Human Body Effects, UAV-Assisted Soldier.

## I. INTRODUCTION

Unmanned aerial vehicles (UAVs) are becoming more ubiquitous due to features such as being lightweight, affordable, and having three-dimensional (3D) maneuverability. With UAVs being integrated in many civilian and military applications such as emergency rescue [1], public safety, remote sensing, target tracking, and intelligence gathering [2], their global market value is expected to reach \$43 billion by 2025 [3]. In a UAV-assisted soldier scenario, for example, the UAV might need to communicate with a device that is either being held or attached to a soldier at altitudes close to the ground. The user could be holding their user equipment (UE) near their chest or inside their pocket with different orientations relative to the UAV. As a result, the wireless channel might go through dramatic changes [4], [5]. Consequently, the optimal placement decision for the UAV, which targets, say, the highest achievable throughput, minimum energy consumption, or maximum flight

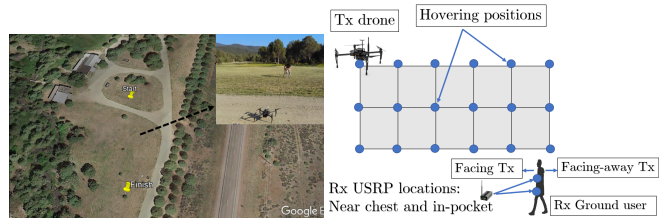


Fig. 1. Top view of the experiment location and an illustration of the investigated use cases for all UAV hovering positions.

time, could depend on the near-body location or user direction. Moreover, due to body-antenna interaction and the near-field coupling effects, antenna radiation patterns can be altered [6], [7], and significant variations in the received signal can be experienced by the user [8]–[10]. While the role of the human body and its effects on terrestrial wireless channels has been the focus of many works, the impact of the user-induced effects on UAV-to-Ground channels has been mostly disregarded in literature. Note that we use Air-to-Ground and UAV-to-Ground interchangeably in this work. The uniqueness of this case study comes from the ability of UAVs to adjust their position in 3D space based on the observed use case. In this work, we show that factors such as UE location and user orientation along with the UAV's 3D location and its antenna radiation pattern have a considerable impact on the wireless channel.

Specifically, we study how three different use cases of holding a UE, namely, Near-Chest Facing (NCF), In-pocket Facing (IPF), and Near-chest Facing-away (NCFA), can affect the UAV-to-Ground channel at ultra-low altitudes (less than 30 m altitude). We measure and analyze how the average received signal strength (RSS), shadowing, and the Rician K-factor are affected by the UAV hovering position, user orientation, and the UE near-body location at carrier frequencies of 900 MHz and 2.5 GHz. This work, to the best of our knowledge, is the first study that characterizes how such channels can be affected chiefly by the user's body.

Our contributions can be summarized as follows:

- We show that, compared to a baseline free-space scenario, the human body near the UE can increase or decrease signal reception, depending on the user's relative orientation to the UAV. Further, these user-induced *gains* and *losses* are found to vary with the UAV hovering position but can reach significant levels (more than 10 dB).
- We experimentally demonstrate how the UAV's hovering position and user orientation can affect shadowing in ultra-low LOS UAV-to-Ground channels. We quantify

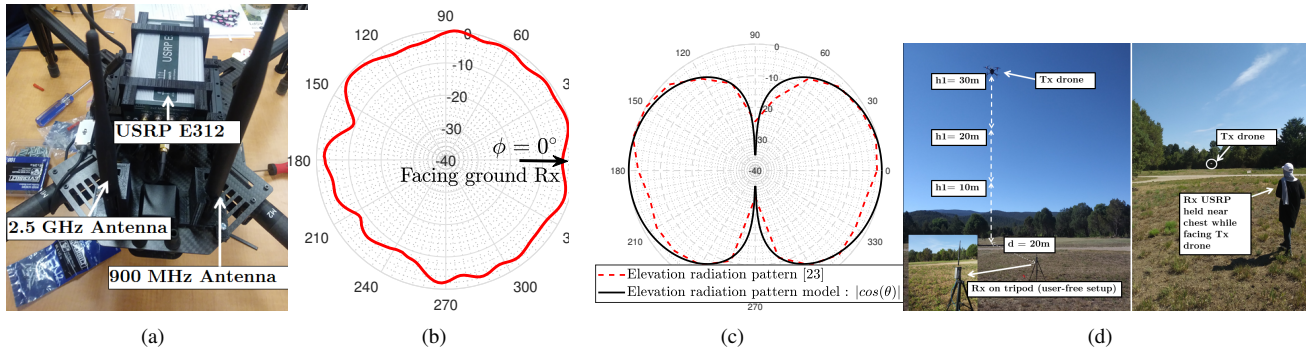


Fig. 2. (a) The used UAV platform with antennas operating at 2.5 GHz and 900 MHz. (b) Azimuth and (c) elevation radiation pattern of the 2.5 GHz antenna. (d) Location and setup for the UAV-to-Ground experiments. The user-free (no human body involvement) setup (left) and NCF setup (right) are shown.

this effect and show that, except for one drone hovering position at which the UAV's body dominates the impact on the channel, shadowing strongly depends on the user body orientation, not the UAV's body nor its location.

- We find that the Rician K-factor depends on the UAV altitude and the user's body. We show that, except for one drone hovering position, the user's body could lead to significant degradation in the K-factor causing an average and a maximum reduction of 6.8 and 15 dB, respectively.

This paper is organized as follows. In Section II, we present our hardware and software setup along with the channel model. Experiment procedures are given in Section III. Baseline, user-free experimental results are discussed in Section IV. We experimentally quantify the user impact on shadowing and average received signal strength in Section V. Section VI describes the Rician K-factor impact. Related work is discussed in Section VII, and conclusions are presented in Section VIII.

## II. SYSTEM DESCRIPTION AND CHANNEL MODEL

### A. Hardware and Software Setup

We use two Universal Software Radio Peripherals (USRP) E312s from Ettus Research™ for recording measurements. The transmitting radio and antenna are mounted on the UAV. The UAV antenna is vertically-mounted and directly connected to the TRX port using an SMB to SMA adapter (Fig. 2(a)). The receiver USRP is either mounted on a tripod, such as the case in the user-free AtG experiments, or being held by the user, which is the case in the human-related experiments. Both radios utilize omni-directional, linearly-polarized antennas (Ettus VERT2450) with a radiation pattern in the azimuth and elevation planes, as shown, respectively, in Figs. 2(b) and 2(c). The transmitter sends a continuous wave (CW) at a sampling rate of 64 kS/s. Measurements are recorded for a period of 20 seconds per hovering position. The processing and analysis is conducted over the middle 15 s to exclude any unwanted UAV transition effects that might occur when the drone is coming to or moving from the desired position. The absolute value of the complex envelope (*i.e.*,  $r = \sqrt{I^2 + Q^2}$ ) is then used for postprocessing. Prior to in-situ field experiments, we calibrated the transmit power at both frequencies of 900 MHz and 2.5 GHz, and quantified the associated cable losses. The Transmit power was 6.2 dBm and the cable loss was 0.4 dB.

### B. Channel Model and Signal Analysis

The channel is assumed to consist of a direct line-of-sight (LOS) component, which might be exposed to different shadowing levels. The channel also consists of multipath components that can constructively or destructively interfere with the direct component, resulting in fast signal fluctuations. Hence, the channel is assumed to have a Rician distribution and it is characterized accordingly. The Rician probability density function is given by [11]:

$$f(r) = \frac{r}{\sigma^2} \exp\left(-\frac{r^2 + a^2}{2\sigma^2}\right) I_0\left(\frac{ra}{\sigma^2}\right), r \geq 0 \quad (1)$$

Here,  $2\sigma^2$  represents the average power of the multipath components,  $a$  denotes the amplitude of the direct component, and  $I_0$  is the Bessel function of the zeroth order. The parameters of the Rician distribution are obtained through the Method of Moments approach [12]. These moments are the mean and standard deviation of the power  $p$ , which is obtained by squaring the normalized absolute value of the complex envelope (*i.e.*,  $p = r^2$ ). Then, we calculate the mean and standard deviation of the power over a window of 4000 samples (which equals 62.5 ms). The window size was empirically selected to satisfy the trade-off between the desire to analyze the shortest time duration possible, to capture small-scale fluctuations, while still remaining statistically meaningful. A similar window size was chosen in our previous work [6]. The windowed mean and standard deviation of power are denoted as  $\mu = \mathbf{E}(W(p_n))$  and  $\eta = \mathbf{E}(W(p_n)) - \mu^2$ , where  $\mathbf{E}$  represented the expectation operation and  $W$  is the windowing operation [13]. From  $\mu$  and  $\eta$ , we then find the Rician distribution parameters for the considered window as follows:  $a^2 = \sqrt{\mu^2 - \eta^2}$ ,  $2\sigma^2 = \mu - \sqrt{\mu^2 - \eta^2}$ . The Rician K-factor per window is then calculated as:

$$K(\text{dB}) = 10 \log_{10} \left[ \frac{a^2}{2\sigma^2} \right] \quad (2)$$

Recall that  $K = -\infty$  dB indicates the absence of a dominant LOS component, resulting in a Rayleigh channel.

## III. EXPERIMENTS DESCRIPTION

We conduct two sets of UAV-to-Ground experiments: one without the human body (user free) and one with a person

holding the UE in different modes. In this section, we explain the procedure for each of these experiment sets.

#### A. User-free UAV-to-Ground Channels

In this scenario, the receiver (Rx) is mounted on a tripod while the transmitter (Tx) is mounted on the UAV. The Tx UAV hovers at three different altitudes from the ground:  $h_1 = 10$  m,  $h_2 = 20$  m, and  $h_3 = 30$  m, and six different horizontal distances that are spaced in 20 m increments starting from  $d_1 = 0$  m (Rx next to Tx), moving to  $d_2 = 20$  m, and so on until it reaches  $d_6 = 100$  m. See Fig. 2(d) for a depiction of the altitudes and experiment location. Measurement collection starts when the UAV hovers above the user at  $d_1$  and altitude  $h_1$ . Then, the UAV changes its horizontal distance from  $d_1$  to  $d_2$  and measurements are collected again. The process is repeated until the UAV reaches  $d_6$  for the same altitude,  $h_1$ . The UAV then moves to  $h_2$ , and the process is repeated until we cover the rest of hovering positions, ending with  $(d_6, h_3)$ . Refer to Fig. 1 for the hovering positions.

#### B. UAV-to-Ground Channels with Different UE Use Cases

Here, we repeat the previous measurements but with a user holding the UE (Rx USRP). The user's weight is 56 kg and their height is 164 cm. We investigate three use cases: (i) Near chest and facing (NCF) towards the Tx UAV, (ii) Near chest and facing-away (NCFA) from the Tx UAV, and (iii) In-pocket while facing (IPF) the Tx UAV. For each use case, we perform AtG experiments at carrier frequencies of 900 MHz and 2.5 GHz, totalling 6 experiment sets. In each of these experiment sets, we analyze how the RSS levels, shadowing, and the Rician K-factor are affected by user orientation, UE near-body location, and the drone's hovering position. An illustration of when a user is facing the Tx UAV while holding the radio device with two hands is shown in Fig. 2(d).

### IV. USER-FREE UAV-TO-GROUND CHANNELS

In this section, we discuss the user-free AtG measurement results, the setup of which is shown in Fig. 2(d) (left). The objective of the experiment is to investigate the UAV-to-Ground channel with no user/human body involvement to directly compare to when a user is holding the UE.

The mean values of the obtained RSS levels at 2.5 GHz are shown in Fig. 3 (in black dashed lines). First, we can see that the results follow a curved shape, which is different from the conventional straight line obtained in ground-to-ground experiments. At  $d = 0$  m (*i.e.*, when the Tx UAV is directly above the Rx), low RSS levels are experienced due to two factors: the antenna elevation radiation pattern (Fig. 2(c)) and the UAV body. Since the Tx and Rx antennas are vertically-mounted, omni-directional antennas, the radiated power is at its minimum value in the vertical direction (*i.e.*,  $\theta = \arctan(\frac{h}{d}) = 90^\circ$ ). As a result, lower RSS levels are recorded at this location compared to other distances/altitudes with angles less than  $90^\circ$ . Furthermore, due to the antenna being mounted on the UAV body, the transmitted signal is shadowed by the UAV body, especially when seen from a node

below. As the Tx UAV moves to subsequent locations, the Rx starts to experience stronger RSS levels due to greater alignment of the radiation pattern and less drone body obstruction. It is interesting to see that for a fixed UAV altitude, the RSS can vary by as much as 20 dB as the UAV moves from directly above the Rx to the next location only 20 m away. This effect is a result of the elevation radiation pattern discussed above.

### V. USER IMPACT ON UAV-TO-GROUND CHANNELS

Here, we investigate how different use cases of holding a UE can affect: (i) average RSS levels, (ii) shadowing, and (iv) the Rician K-factor of an AtG channel at various UAV altitudes, locations, and carrier frequencies. In doing so, we consider the relative impact of user versus UAV properties on the resulting wireless channel characteristics at ultra-low drone altitudes.

#### A. Average RSS and User-induced Loss/Gain

We define the user-induced loss/gain as the difference in RSS between the baseline (User-free) scenario and the facing and facing-away scenarios when the user holds the UE close to the chest. Fig. 3(a) shows the average RSS for these three scenarios (user-free, NCF, and NCFA), which we now analyze.

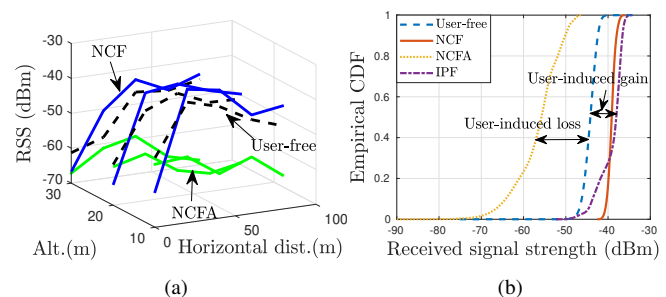


Fig. 3. (a) Average RSS levels for the user-free, NCF, and NCFA scenarios at 2.5 GHz. (b) The empirical CDF for all investigated cases at  $(d_2, h_2)$

**User-Induced Gain Compared to Free Space.** To investigate how the existence of the human body can affect the UAV-to-Ground channel, we first compare the results of the Near-Chest Facing (NCF) scenario to those obtained in the user-free experiment. Visually, this comparison could be made by inspecting Fig. 3(a). We find that the body of the user when facing the transmit UAV can actually result in *increased* RSS levels. For example, while the mean RSS level at  $(d_5, h_1)$  is  $-46.2$  dBm in the user-free setup, it is  $-40.3$  dBm when the user holds the UE facing the transmit UAV (*i.e.*, NCF), a 5.8 dB increase in the mean RSS. At the location of  $(d_2, h_3)$  a 7.6 dB increase in the mean RSS level is experienced due to the existence of the user's body. Similar results are found when the UE is inside the user's pocket. We have previously observed this effect in a Ground-to-Ground channel, where the user's body resulted in a 14% increase in throughput over a user-free setup [5]. However, it is worth noting here that the above finding depends on the UAV hovering position. For example, at 0 m horizontal distance (*i.e.*, UAV directly above user), the existence of the user's body and orientation becomes almost irrelevant to the average RSS changes as the gain/loss compared to the baseline are minimal (less than a

standard deviation). Other works have also shown that the human body can increase the radiation of the antennas and additional gains of 15 dB were measured compared to free space [10]. We conclude that, compared to a user-free scenario, there exists a user-induced *gain* that increases the RSS when the UE is facing a transmitting, in-flight drone when a LOS path exists from sender to receiver. The average and maximum *gain* across all locations at 2.5 GHz was 3.4 dB and 12.05 dB, respectively. Finally, we report that with the exception of three hovering positions, average user-induced gains compared to free space at 900 MHz were insignificant, *i.e.*, less than the standard deviation of the measured signal. This result might be due to the fact that the human body absorbs more power at low frequencies compared to higher frequencies at which it can reflect more power [14]. A similar effect is shown in [15], where three different human bodies were studied at 17 different frequencies.

**User-Induced Loss Compared to Free Space.** Next, we quantify the role of the human body on the channel when the user's orientation changes (*i.e.*, the whole body is in the path of the signal). To do so, we compare the measured RSS in the Near-Chest Facing-away (NCFA) scenario to those obtained in the baseline (User-free) setup. We find that the user's body indeed causes reductions in the average RSS, which is clear via visual inspection of Fig. 3(a). In particular, if we exclude the strictly-vertical UAV position at which the user's orientation is virtually irrelevant, the user's body is found to considerably reduce the average RSS. At 2.5 GHz, an average reduction of 13.2 dB and a maximum reduction of 23.1 dB across all drone hovering positions is experienced. An example of this loss at  $(d_2, h_2)$  is shown in Fig. 3(b) with an average value of 12.3 dB. Higher loss is measured at 900 MHz, with an average and maximum reduction of 17.5 dB and 26.3 dB, respectively. This result is in line with the finding above as the human body involved in this study is found to result in more attenuation (most likely through absorption) at this frequency than at 2.5 GHz.

**Impact of User Orientation.** Now that we understand how the user's body can affect the channel compared to a free-space baseline, it is interesting to compare, for the same person, how their orientation and the near-body location of the UE can affect the UAV-to-ground channel. First, we compare the NCFA measurements to those obtained in the NCF scenario. The results of this comparison are plotted in terms of the average difference across distances at 900 MHz (Fig. 4(a)) and across altitudes for the two frequencies (Fig. 4(b)). The human body results in signal blockage and substantial losses reaching an average value (across altitudes) of up to 21.6 dB at 2.5 GHz, and 18.6 dB at 900 MHz. However, this observation does not apply to the strictly-vertical location, where user orientation is arbitrary relative to the UAV. In fact, for that case, the NCFA sometimes results in higher RSS levels as the user and UAV-mounted antennas are facing the same direction. See Fig. 4(b), where the two solid lines are less than or equal to 0 dB.

**Impact of Near-Body Location for a Fixed User Orientation.** For the same drone hovering position and the same

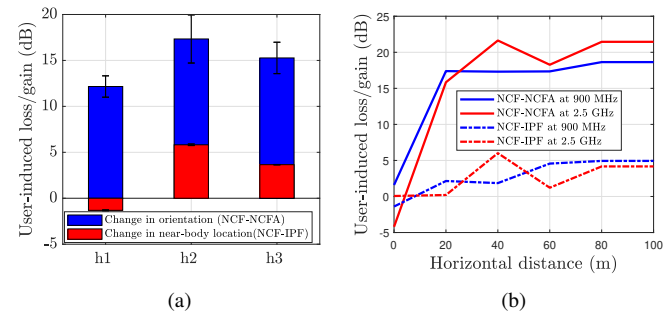


Fig. 4. User-induced impact due to orientation and UE near body location. Average over: (a) distances at specific heights (900 MHz), and (b) heights at specific horizontal distances (both frequencies).

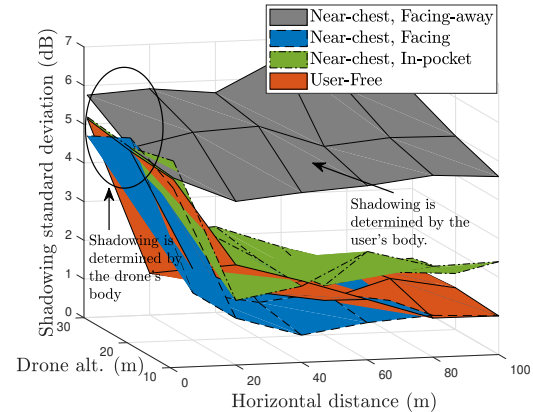


Fig. 5. Shadowing standard deviation for all investigated use cases at 2.5 GHz.

user orientation of facing the transmit UAV, we investigate if placing the UE near different body locations yields different received signal strengths. To do so, we calculate the difference in average RSS level in the NCF and the IPF scenarios and analyze the results. This difference at 900 MHz is plotted in red in Fig. 4(a) as an average over all distances for each altitude. First, we see that placing the UE inside the pocket reduces the average RSS levels at  $h_2$  and  $h_3$ , by up to 6 dB. However, at the lower altitude of  $h_1$ , the in-pocket scenario results in higher average RSS levels. For example, at  $(d_3, h_1)$  (not shown here) we measure an average of 3.2 dB higher RSS when inside the pocket compared to near the chest. The average difference over all distances is -1 dB (see Fig. 4(a)). This improvement could be attributed to the fact that, as the drone hovers at lower altitudes, it starts to exhibit a stronger LOS with the UE inside the pocket, and as a result, the difference between the two use cases decreases. Recalling that the user's orientation is fixed (facing the UAV), we conclude that there exists not only an optimal UAV position for a UAV-to-user connectivity based on their orientation, but there also exists an optimal UE location on/near their body when facing the UAV in a LOS setup.

### B. Shadowing Due to UAV and User Bodies

In this section, we analyze how the shadowing standard deviation, denoted as  $\sigma_s$ , is affected by the UAV, its mounted antenna radiation pattern, and the human body.

We have investigated the shadowing standard deviation for all experiments and found that it is greatest when the UAV is

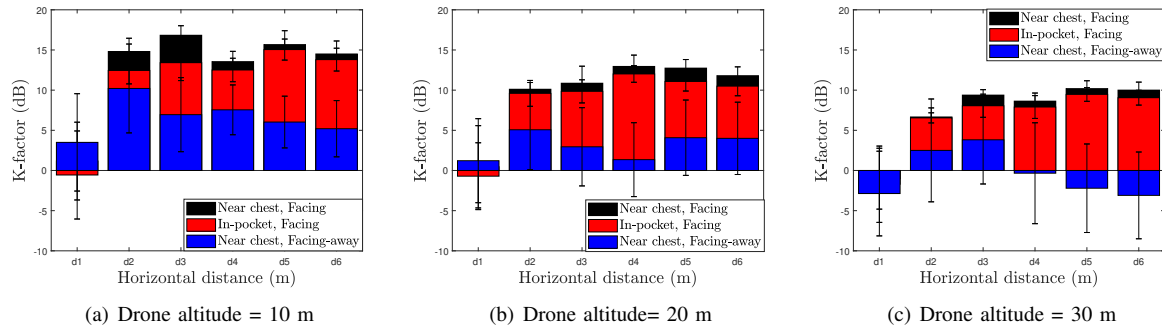


Fig. 6. The average and standard deviation of the measured Rician K-factor for the three use cases of the LOS UAV-to-Ground channel at 2.5 GHz.

directly above the user (at  $d_1$ ) with values of  $\sigma_s > 4$  dB across all experiments and frequencies. Then, it gradually decreases as the UAV moves to more-distant locations that have a less obstructed Tx-Rx path. This behavior occurs in both scenarios of facing and in-pocket, and it can be clearly seen in Fig. 5, where we plot  $\sigma_s$  for all UAV locations at 2.5 GHz. In this figure, we can see that shadowing is approximately the same for the three use cases when the UAV is above the user at  $d_1$  for all altitudes. At this UAV hovering position, shadowing is dominated by the UAV's body, not the user or their orientation. Moving away from this location, shadowing starts to decrease for the facing and in-pocket scenarios while, in the facing-away scenario, it stays approximately the same regardless of the UAV location, suggesting that *shadowing becomes dominated by the user's body, not the UAV.*

## VI. THE RICIAN K-FACTOR IN UAV-TO-GROUND CHANNELS FOR DIFFERENT USE CASES

In this section, we present how the Rician K-factor, which measures the channel fading severity, depends on the user orientation, UE near-body location, and UAV hovering location.

### A. Rician K-factor When Facing Tx UAV

The average and standard deviation of the K-factor at 2.5 GHz across all locations and use cases are shown in Fig. 6.

First, we see that, for the same altitude, the Rician K-factor experiences a significant change as the UAV moves from  $d_1$  to any other hovering position. For example, in Fig. 6(a), when in-pocket and at a UAV altitude of 10 m, the average K-factor can change from approximately  $\bar{K} = 0$  dB, when the Tx UAV is directly above the ground Rx (*i.e.*,  $d_1 = 0$  m), to  $\bar{K} = 12$  dB, as the UAV hovers at  $d_2 = 20$  m. Such a dramatic change in the K-factor is attributed to the impact of both the elevation radiation pattern of the vertically-oriented antenna and the body of the UAV. Recall that a vertically-oriented omni-directional dipole antenna theoretically does not radiate in the vertical direction. In reality, however, there will still be some radiated power at significantly-less levels. This radiation-pattern effect will impact the main LOS component of the received signal, while the body of the UAV and its induced reflections will cause a larger value for the multipath component ( $\sigma$  in (2)). The end result of this effect is the significant reduction in the K-factor, which we observed at  $d_1$  at all altitudes and both carrier frequencies.

TABLE I  
AVERAGE K-FACTOR LOSS ( IN DB) RELATIVE TO NCF SCENARIO.

Altitude	NCF	IPF
$h_1$ (10 m)	6.18	1.64
$h_2$ (20 m)	6.70	1.09
$h_3$ (30 m)	7.67	0.75

### B. Rician K-factor when Facing-away from Tx UAV

We find that in all but one location, where the UAV hovers directly above the user, the K-factor reduces significantly as the user faces-away from the UAV. This reduction is clear in the results plotted in Fig. 6. At  $h_1$ , for example, the difference in K-factor between the NCF and NCFa scenarios can reach up to 11 dB and has an average value across all locations of 6.18 dB. As the UAV moves to higher altitudes and the general trend of the K-factor tends to result in weaker values for all scenarios, the user's body blockage starts to result in negative values (in dB) at  $h_3$ , suggesting an extremely weak LOS component and an increase in multipath effects. The average K-factor loss across all hovering positions due to placing the UE in-pocket (IPF) or facing-away from the UAV (NCFa) are summarized in Table I.

## VII. RELATED WORK

The work in [7], which targets the same issue investigated here, studies ultra-low UAV-to-Ground channels for three different environments and two user modes: texting and calling. Measurements and analysis were carried out for a limited drone path of 20 m with an emphasis on the impact of the environment on the channel rather than on the human body. Autonomous QoS-driven UAVs in air-to-ground channels are prototyped and experimentally investigated for three ground devices that were not held by humans in [16]. The work in [17] studies drone-to-ground channels for a tripod-mounted receiver. The work in [24] characterizes the K-factor for low-altitude UAVs in urban environments crowded with buildings and spanned large horizontal distances. A statistical channel model is proposed to capture the effects of the human body on RSS in [18]. Furthermore, the human body impact has been the focus of many research works. User-induced effects on shadowing were investigated at 2.45 GHz in stationary, rotating, and mobile scenarios in [19]. Losses due to human blockage of up to 20 dB were reported in [26]. In [5], [10], [15], [25] it was shown that the human body can act as an antenna and result in increased received signal levels compared

to free space. A machine learning approach that distinguishes between different indoor user modes was proposed in [20]. Lastly, some works, such as [21], [22] have studied optimizing UAV-to-user channels but excluded the human-induced effects which we show here to be non-negligible. Our study emphasizes the impact of the human body on such channels bringing experimental insight otherwise missing to the topic.

### VIII. CONCLUSION

We have experimentally shown how the human body and different use cases of holding a UE affect the LOS UAV-to-Ground channel at ultra-low altitudes. First, compared to a scenario where the receiver node is mounted on a tripod in free space, the human body is shown to result in gains/losses depending on the user's orientation relative to the transmitting UAV. Second, we show that, depending on the drone's hovering position, there are two distinct regions for shadowing: One that is dominated by the drone body and another that is strongly dependent on the user's orientation. Third, we show that the Rician K-factor is not only a function of altitude, but strongly depends on user orientation with reductions in the average value reaching 15 dB at some drone hovering positions. We intend to leverage our dataset and the insight drawn from this work to build a machine learning framework that enables UAVs to dynamically adjust their hovering position to optimize for a certain performance metric, whether it is throughput, reliability, or flight time.

### IX. ACKNOWLEDGEMENT

This work was supported in part by the NSF via grants CNS-1823304 and CNS-1909381 and in part by the Air Force Office of Scientific Research via grant FA9550-19-1-0375.

### REFERENCES

- [1] Canadian Drone Test Uses LTE Network to Deliver Defibrillators, Ericsson website: <https://www.ericsson.com/en/news/2019/10/defibrillators-delivered-via-lte-enabled-drones-in-canada>.
- [2] V. Chamola, P. Kotes, A. Agarwal, Naren, N. Gupta, and M. Guizani, "A Comprehensive Review of Unmanned Aerial Vehicle Attacks and Neutralization Techniques," *Ad Hoc Networks*, p. 102324, 2020
- [3] The drone market, Drone Industry Insights, website: <https://droneii.com/the-drone-market>.
- [4] V. Plicanic, B. K. Lau, A. Derneryd, and Z. Ying, "Actual diversity performance of a multiband diversity antenna with hand and head effects," in *IEEE Trans. Antennas Propag.*, vol. 57, no. 5, May 2009.
- [5] Y. Shi, J. Wensowitch, E. Johnson, and J. Camp, "A Measurement Study of User-Induced Propagation Effects for UHF Frequency Bands," in *Proc. of IEEE SECON*, June 2017.
- [6] M. Badi, J. Wensowitch, D. Rajan, and J. Camp, "Experimentally Analyzing Diverse Antenna Placements and Orientations for UAV Communications," in *IEEE Trans. Veh. Technol.* vol. 69, no. 12, Dec. 2020.
- [7] P. A. Catherwood et. al., "Radio Channel Characterization of Mid-Band 5G Service Delivery for Ultra-Low Altitude Aerial Base Stations," in *IEEE Access* 7: 8283-8299, Jan. 2019.
- [8] N. Amani, V. Dehghanian, and J. Nielsen, "User-induced antenna variation and its impact on the performance of RSS-based indoor positioning," in *Proc. IEEE Can. Conf. Elect. Comput. Eng. (CCECE)*, May 2016.
- [9] S. Shikhantsov, A. Thielens, G. Vermeeren, P. Demeester, L. Martens, G. Torfs, and W. Joseph, "Massive MIMO Propagation Modeling With User-Induced Coupling Effects Using Ray-Tracing and FDTD," in *IEEE J. Sel. Areas Commun.*, Sep. 2020.
- [10] M. Heino, C. Icheln, and K. Haneda, "Self-user shadowing effects of millimeter-wave mobile phone antennas in a browsing mode," in *Proc. 13th European Conf. on Antennas and Propag. (EuCAP)*, March 2019.
- [11] A. Goldsmith, *Wireless Communications*. Cambridge, U.K.: Cambridge Univ. Press, 2005
- [12] L. Greenstein, D. Michelson, and V. Erceg, "Moment-method estimation of the Rician K-factor," in *IEEE Commun. Lett.*, vol. 3, June 1999.
- [13] M. Simunek, F. P. Fontan, and P. Pechac, "The UAV low elevation propagation channel in urban areas: Statistical analysis and time-series generator," in *IEEE Trans. Antennas Propag.*, vol. 61, no. 7, Jul. 2013.
- [14] C.W.Kim and T.S.P.See, "Rf transmission power loss variation with abdominal tissues thicknesses for ingestible source," in *e-Health Networking Applications and Services (Healthcom)*, 2011 13th IEEE International Conference on, Jun 2011, pp. 282–287.
- [15] E.Cabot, I. Stevanovic, N. Kuster, and M. H. Capstick, "A numerical assessment of the human body effect in the transmission of wireless microphones," in *Microwave and Optical Technology Letters*, vol. 61, no. 3, Mar 2019. Available: [https://d24z4d3zypmncx.cloudfront.net/KnowledgeBaseFiles/effect\\_human\\_body\\_wireless\\_mic\\_transmission.pdf](https://d24z4d3zypmncx.cloudfront.net/KnowledgeBaseFiles/effect_human_body_wireless_mic_transmission.pdf)
- [16] L. Ferranti et al., "SkyCell: A Prototyping Platform for 5G Aerial Base Stations," in *Proc. IEEE WoWMoM*, Sep. 2020.
- [17] Y. Shi, R. Enami, J. Wensowitch, and J. Camp, "Measurement-Based Characterization of LOS and NLOS Drone-to-Ground Channels," in *Proc. of IEEE WCNC - PHY and Fundamentals*, Barcelona, Spain, April 2018.
- [18] M. Mohamed, M. Cheffena, A. Moldsvor, and F. P. Fontan, "Physical statistical channel model for off-body area network," in *IEEE Antennas Wireless Propag. Lett.*, vol. 16, Jan. 2017.
- [19] S. Cotton, A. McKernan, A. Ali, and W. Scanlon, "An experimental study on the impact of human body shadowing in off-body communications channels at 2.45 ghz," in *Proc. 5th European Conf. on Antennas and Propag. (EuCAP)*, April 2011.
- [20] L. Zhang et. al., "An RSS-based classification of user equipment usage in indoor millimeter wave wireless networks using machine learning," in *IEEE Access*, vol. 8, Jan. 2020.
- [21] Q. Wu, J. Xu, and R. Zhang, "Capacity characterization of UAV-enabled two-user broadcast channel," *IEEE J. Sel. Areas Commun.*, Aug. 2018.
- [22] S. Ahmed, M. Z. Chowdhury, and Y. M. Jang, "Energy-efficient UAV-to-user scheduling to maximize throughput in wireless networks," *IEEE Access*, vol. 8, Jan. 2020.
- [23] Data-sheet and anechoic chamber measurements results for co-polarized and cross-polarized links in the elevation and azimuth planes for VERT antennas. <https://smu.box.com/s/wmq2xf8fiefd5pwse88w60an8vy7jmm>
- [24] J. Rodríguez-Piñero et al., "Air-to-Ground Channel Characterization for Low-Height UAVs in Realistic Network Deployments," in *IEEE Trans. Antennas Prop.*, vol. 69, no. 2, Feb. 2021.
- [25] B. Kibret, A. K. Teshome, and D. T. H. Lai, "Characterizing the human body as a monopole antenna," *IEEE Trans. Antennas Propag.*, vol. 63, no. 10, pp. 4384–4392, Oct. 2015
- [26] Ł. Januszkiwicz, "Analysis of human body shadowing effect on wireless sensor networks operating in the 2.4 ghz band," *Sensors*, vol. 18, no. 10, p. 3412, 2018